Kishida et al., Int J Cardiovasc Res 2016, 5:1
http://dx.doi.org/10.4172/2324-8602.1000252

International Journal of Cardiovascular Research

Research Article

A SCITECHNOL JOURNAL

# Short-Term Treatment with an Angiotensin II Receptor Blocker Prevents Necrotic Core Formation by Inhibiting Oxidative Stress-Mediated Apoptosis in Macrophages

**Sou Kishida, Hiroyuki Yamada*, Noriyuki Wakana, Hiroyuki Kawahito, Daisuke Irie, Taku Kato, Masakazu Kikai, Kensuke Terada, Keita Yamamoto, Naotoshi Wada, Shinichiro Motoyama, Hiroki Takata, Hirokazu Yokoi, Yoshinori Tsubakimoto, Takehiro Ogata, Tomomi Ueyama and Satoaki Matoba**

**Abstract**

**Objective:** To study the role of angiotensin II (Ang II) type 1 receptor (AT1R) on necrotic core formation associated with endoplasmic reticulum (ER) stress-induced macrophage apoptosis.

**Methods and Results:** Eight-week-old ApoE-deficient mice were fed a high-cholesterol diet and administered AT1R blocker (ARB), hydralazine, or vehicle from 15 weeks of age. Histochemical analysis of brachiocephalic artery at 19 weeks of age showed a marked reduction of necrotic core area in ARB-treated mice. At 17 weeks of age, mRNA expression levels of C/EBP Homologous Protein (CHOP) and the percentage of TUNEL-positive cells were also decreased in ARB-treated mice, concomitant with the significantly lower expressions of NOX2 and NOX4 genes. Free cholesterol (FC)-loaded thioglycollate-induced peritoneal macrophages (TGPM) showed a significant increase in CHOP mRNA expression and the number of annexin V- or propidium iodide (PI)-positive cells; however, these were not affected by cotreatment with Ang II or Ang II plus ARB. In contrast, TGPM isolated from Ang II-treated mice, exhibiting higher expression levels of NOX2 and $p22^{phox}$ genes, showed a more robust increase in CHOP mRNA expression after FC loading.

**Conclusions:** Our findings demonstrate that ARB treatment inhibits necrotic core formation, in part by alleviating oxidative stress-mediated amplification of ER stress-induced macrophage apoptosis.

**Keywords**

Atherosclerosis; Renin angiotensin system; Endoplasmic reticulum stress; Apoptosis; Macrophage; Oxidative stress; CHOP; Necrotic core

***Corresponding author:** Hiroyuki Yamada, Department of Cardiovascular Medicine, Graduate School of Medical Science, Kyoto Prefectural University of Medicine, 465 Kajii-cho, Kamigyo-ku, Kyoto, 602-8566 Japan. Tel: +81-75-251-5511; Fax: +81-75-251-5514; E-mail: hiyamada@koto.kpu-m.ac.jp

**Received:** November 03, 2015 **Accepted:** January 03, 2016 **Published:** January 11, 2016

## Introduction

The renin-angiotensin system (RAS) is profoundly involved both in atherosclerotic lesion initiation as well as advanced plaque progression in both animal experiments and human studies of atherosclerosis [1-4]. Treatment with angiotensin II type 1 receptor (AT1R) blocker (ARB) has been reported to inhibit the progression of vulnerable plaque [5-9]; however, the mechanisms underlying this beneficial effect of ARB in reducing the vulnerability of advanced atherosclerotic plaque, especially in terms of necrotic core formation, have not been fully investigated.

Macrophage apoptosis substantially contributes to necrotic core expansion in advanced plaques [10-14], which is accompanied by augmented accumulation of macrophages, thinned fibrous cap, and enhanced proinflammatory response, resulting in plaque disruption and ultimately in acute atherothrombolic vascular disease [15-17]. Endoplasmic reticulum (ER) stress has been profoundly implicated in macrophage apoptosis [18-21]. When ER stress is abnormally prolonged, C/EBP homologous protein (CHOP) is upregulated in plaque lesions, triggering plaque necrosis [22-25]. CHOP-deficient atherosclerosis-prone mice showed a significant reduction in apoptosis and subsequent plaque necrosis [23]. Furthermore, Miyoshi et al. reported a striking relationship between advanced lesion stage, CHOP expression, and apoptosis in human coronary artery lesions [22].

Recent studies have demonstrated that RAS plays a crucial role in the pathogenesis of ER stress-related cardiovascular diseases, such as congestive heart failure, cardiac remodeling after myocardial infarction, and renal disease [26-28]. Although RAS is largely involved in the pathogenesis of atherosclerosis, its effect on ER stress in the context of the development of vulnerable plaque has not been fully elucidated. In this study, we examined the role of RAS in ER stress-related atherosclerotic lesion development using *in vivo* plaque rupture model. In additional *in vitro* experiments, we show the possibility that while AT1R is not autonomously involved in ER stress-induced macrophage apoptosis; it amplifies ER stress-induced macrophage apoptosis by enhancing oxidative stress. Our findings suggest that oxidative stress is a potential therapeutic target to reduce ER stress-induced macrophage apoptosis and stabilize advanced atherosclerotic plaques.

## Methods

### Experimental animals

All experiments were performed in strict adherence to the "Directive 2010/63/EU" of the European Parliament and to the Guidelines for Animal Experiments of the Kyoto Prefectural University of Medicine, following approval by a local university ethics review board.

Apolipoprotein E deficient ($ApoE^{-/-}$) mice (C57BL/6) were obtained from Taconic Co., Ltd. (Germantown, NY, USA). Eight-week-old male $ApoE^{-/-}$ mice were fed a high-cholesterol diet (13.6% fat, 1.25% cholesterol; Oriental Yeast Co., Tokyo, Japan). From 15 weeks of age, ARB (olmesartan, 3 mg/kg/day), hydralazine (50 mg/kg/day), or saline were administered using an osmotic minipump until 19 weeks of age. For implantation of an osmotic minipump, mice

were anesthetized using isoflurane (2%, 0.2 mL/min) throughout the surgery. The depth of anesthesia was confirmed by lack of tail pinch response. The animals were housed in a room maintained at 22°C under a 12-hr light/dark cycle and were provided with drinking water *ad libitum*. At 19 weeks of age, the area of the atherosclerotic lesion in the brachiocephalic artery was evaluated. Before harvesting the tissues, mice were euthanized by trans-cardiac perfusion under anesthesia induced by isoflurane.

### Hemodynamic analysis

Systolic blood pressure and heart rates were measured under conscious and unrestrained conditions using a programmable sphygmomanometer (BP-98A; Softron, Tokyo, Japan).

### Serum lipid analysis

Measurements of total cholesterol, triglyceride, low density lipoprotein cholesterol, and high density lipoprotein cholesterol were outsourced to SRL, Tokyo, Japan.

### Quantitative analysis of atherosclerotic lesions

Mice were euthanized, and brachiocephalic arteries were embedded in paraffin. Sections were cut every 100 μm along the brachiocephalic artery from the proximal end. Atherosclerotic lesions were examined at 3 different locations. Imaging and analysis of Miller's elastin/van Gieson-stained artery was accomplished using Image J Software (http:rsbweb.nih.gov/ij/).

### Immunohistochemistry

Brachiocephalic artery was quickly removed after PBS perfusion, embedded in paraffin, and immunofluorescently labeled. For Mac-2 staining, a combination of anti-mouse Mac2 antibody (CEDARLANE, Burlington, Ontario, Canada) and Alexa Flour 488-conjugated secondary antibodies (Invitrogen, Carlsbad, California, USA) was used. Apoptosis in atherosclerotic lesions was detected by terminal deoxynucleotidyl transferase dUTP nick end labeling (TUNEL) staining using the tetramethylrhodamine red *in situ* cell death detection kit (Roche) following the manufacturer's protocol. Nuclei were labeled using DAPI solution (DOJINDO, Kumamoto, Japan). The TUNEL-stained sections were analyzed using a LSM 510 META confocal microscope (Carl Zeiss, Jena, Germany), and quantification was performed using Image J. Non-immune immunoglobulin and Alexa Flour 488-conjugated secondary antibodies (Invitrogen, Carlsbad, California, USA) were used as negative controls. The numbers of Mac2-positive or TUNEL-positive cells were assessed using data collected from 3 sections of each animal (6 animals in each group).

### Real-time PCR

Total RNA was extracted from brachiocephalic artery and reverse-transcribed to prepare cDNA. Real-time PCR was performed on a Thermal Cycler Dice (Takara Bio, Shiga, Japan), using SYBR Premix Ex Taq 2 (Takara Bio, Shiga, Japan). Dissociation curves were examined for aberrant formation of primer dimers. PCR-amplified products were electrophoresed on 2% agarose gels to confirm the presence of a single amplicon. Data were expressed as gene expression levels relative to those of the control.

### Free cholesterol (FC)-induced apoptotic response in thioglycollate-elicited peritoneal macrophages (TGPMs)

Peritoneal exudate cells were harvested from the peritoneal cavities of wild-type mice 4 days after an intra-peritoneal injection of 2.0 mL of 3% sterile thioglycollate medium. After 3 h of incubation in Dulbecco's Modified Eagle's Medium (DMEM) containing 10% FBS, non-adherent cells were removed and fresh medium was added. Flow cytometric analysis showed that more than 90% of the adherent cells were positive for F4/80.

After 24 hours, cells were incubated with 100 μg/mL acetyl-LDL (Biomedical Technologies Inc., Stoughton, MA) plus the acyl-CoA:cholesterol acyltransferase inhibitor CI976 (Sigma-Aldrich Inc; 10 μmol/L) alone or with Ang II ($10^{-7}$ M). Olmesartan ($10^{-5}$ M) or PD123319 ($10^{-5}$ M) was added 2 h prior to stimulation. When isolating TGPM from Ang II-treated wild-type mice, a peritoneal injection of 1 mL of Ang II ($10^{-7}$ M) was performed 24, 21, and 18 h prior to cell harvesting, as described previously [29]. After the indicated incubations, 100 μl of 1 x annexin-binding buffer (25 mM HEPES, 140 mM NaCl, 1 mM EDTA, pH 7.4, 0.1% bovine serum albumin) containing 5 μl of Alexa-488 annexin V, 1 μl of 100 μg/ml propidium iodide (PI), and hoechst dye were added to the cells for 15 min at room temperature according to the manufacturer's instructions (Molecular Probes). Cells were viewed with a 40 x objective using a LSM 510 META confocal microscope (Carl Zeiss, Jena, Germany), and quantification was performed using Image J. Five fields of cells for each condition (~1000 cells) were counted. In this protocol, apoptosis is defined as those cells that stain with annexin V or PI, and the data are expressed as the percentage of these cells per total cells counted.

### Statistical analysis

All data are expressed as mean ± SE. Mean values were compared using ANOVA. If a statistically significant effect was found, Tukey-Kramer test was performed to analyze the differences between the groups. $P<0.05$ was considered statistically significant.

## Results

### Necrotic core formation is significantly reduced in ARB-treated ApoE$^{-/-}$ mice

In preliminary experiments, we examined the atherosclerotic lesions in the brachiocephalic arteries of 16- and 20-week-old ApoE$^{-/-}$ mice fed a high-cholesterol diet from 8 weeks of age. Consistent with the previous findings of Johnson et al. [30], the necrotic core area was found to have extensively expanded from 16 weeks to 20 weeks of age (Supplemental Figure 1). To examine the effect of ARB treatment on the expansion of necrotic core area, olmesartan, hydralazine, or vehicle was administered from 15 weeks of age. At 19 weeks of age, ARB-treated mice showed a marked reduction in the necrotic core area as well as the atherosclerotic plaque area compared with hydralazine- and vehicle-treated mice (Figure 1A and 1B). Lipid profile did not differ between the 3 groups except for high-density lipoprotein cholesterol (Supplemental Figure 2A). Compared to vehicle-treated mice, systolic blood pressure was significantly decreased in ARB- and hydralazine-treated mice; however, there was no significant difference between the 2 groups (Supplemental Figure 2B), suggesting that the inhibitory effect of ARB on necrotic core expansion was independent of its antihypertensive effect. The number of MAC-2-positive cells as well as CD68 mRNA expression levels at 17 weeks of age was significantly reduced in ARB-treated mice accompanied by the decreased mRNA expression of MCP-1 (Figures 1C and 1D), suggesting that ARB treatment attenuates

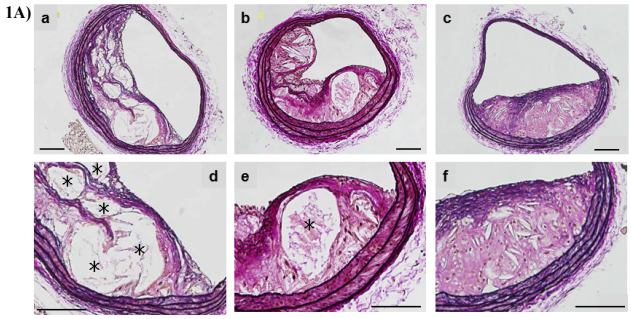


**Figure 1A: Necrotic core expansion is markedly inhibited in ARB-treated 19-week-old ApoE$^{-/-}$ mice.**
**(A)** Representative photographs of Elastica van Gieson-stained brachiocephalic artery in ApoE$^{-/-}$ mice fed a Western diet for 11 weeks from 8 weeks of age. Control mice (a,d), hydralazine-treated mice (b,e), ARB-treated mice (c,f). * indicates necrotic core. The scale bar shows 100-μm intervals.

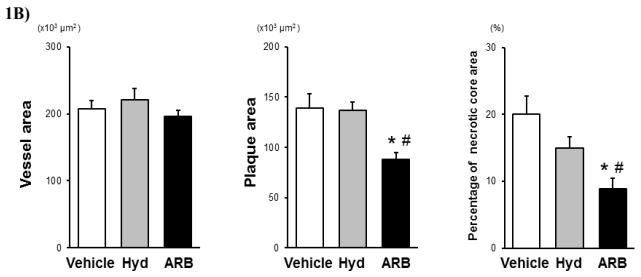


**Figure 1B:** Quantitative analysis showing a significant reduction in atherosclerotic lesion area and percentage of necrotic core area in ARB-treated mice compared with hydralazine-treated and vehicle-treated mice. Values are the mean ± SE for 15 (vehicle), 11 (hydralazine), and 17 (ARB) mice in each group. *P<0.05 vs. vehicle-treated mice. #P<0.05 vs. hydralazine-treated mice. Hyd: hydralazine. ARB: angiotensin receptor blocker.

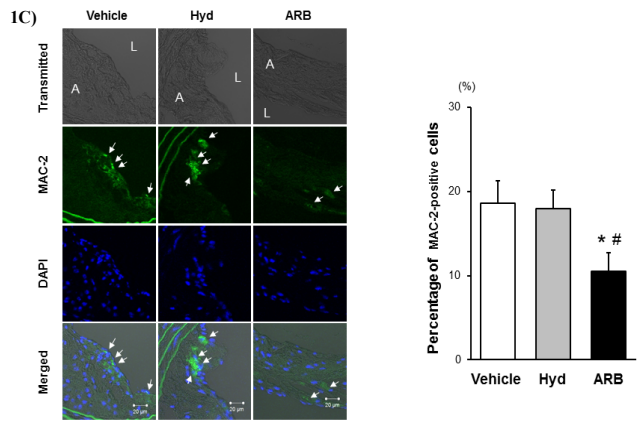


**Figure 1C:** Immunohistochemical staining and quantitative analysis of Mac-2-positive cells. Each group consisted of 3 (vehicle), 4 (hydralazine), and 5 (ARB) mice in each group. *P<0.05 vs. vehicle-treated mice. #P<0.05 vs. hydralazine-treated mice. Hyd: hydralazine. ARB: angiotensin receptor blocker. Arrow indicates Mac-2-positive cells. The scale bar shows 20-μm intervals.

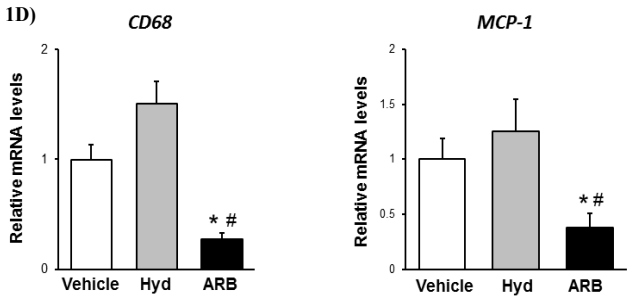


**Figure 1D:** Quantitative PCR analysis of the mRNA expression levels of CD68 and MCP-1 in the brachiocephalic artery of 17-week-old ApoE$^{-/-}$ mice. Values are the mean ± SE relative to those in vehicle-treated mice. Each group consisted of 7 (vehicle), 4 (hydralazine), and 6 (ARB) mice in each group. *P<0.05 vs. vehicle-treated mice. #P<0.05 vs. hydralazine-treated mice. Hyd: hydralazine. ARB: angiotensin receptor blocker. MCP-1: monocyte chemotactic protein-1.

the migration of monocytes/macrophages into the atherosclerotic plaque lesions preceding the necrotic core expansion.

## TUNEL-positive cell numbers are markedly reduced in ARB-treated ApoE$^{-/-}$

To examine the effect of ARB treatment on apoptosis in atherosclerotic plaque, TUNEL staining was performed at 17 weeks of age as it would have been difficult to detect apoptotic cells after the formation of the large necrotic core was completed. As expected, ARB-treated mice showed a marked decrease in the percentage of TUNEL-positive cells compared with hydralazine- and vehicle-treated mice (Figures 2A and 2B), suggesting that the inhibitory effect of ARB on plaque apoptosis contributes to the reduced necrotic core expansion in ARB-treated mice.

## CHOP mRNA expression is markedly inhibited in ARB-treated ApoE$^{-/-}$ mice

We next examined the mRNA expression levels of CHOP and B-cell lymphoma 2 (Bcl-2), which are involved in apoptosis in atherosclerotic lesions. Although Bcl-2 mRNA expression level was not increased in ARB-treated mice, CHOP mRNA expression level was significantly lower in ARB-treated mice than those in hydralazine- and vehicle-treated mice (Figure 3A), suggesting that ARB treatment inhibits ER stress-induced apoptosis by reducing CHOP mRNA expression. We tried to examine the protein expression levels in the brachiocephalic arteries; however, the amount of protein lysates was too small to perform a conventional Western blotting. Activation of AT1R has been reported to increase oxidative stress [31-33], and CHOP expression is augmented by oxidative stress [34-36]. We therefore examined the mRNA expression levels of Nox2 and Nox4, which encode key NADPH oxidases involved in intracellular reactive oxygen species (ROS) production [32,35]. The mRNA expression levels of Nox2 and Nox4 were markedly reduced by ARB treatment (Figure 3B). These findings suggest that amelioration of oxidative stress by ARB treatment may contribute to the inhibition of ER stress-induced apoptosis in ARB-treated mice.

## Cotreatment with Ang II does not increase CHOP mRNA expression and subsequent apoptosis in FC-loaded peritoneal macrophages

We further examined whether AT1 receptor activation and its

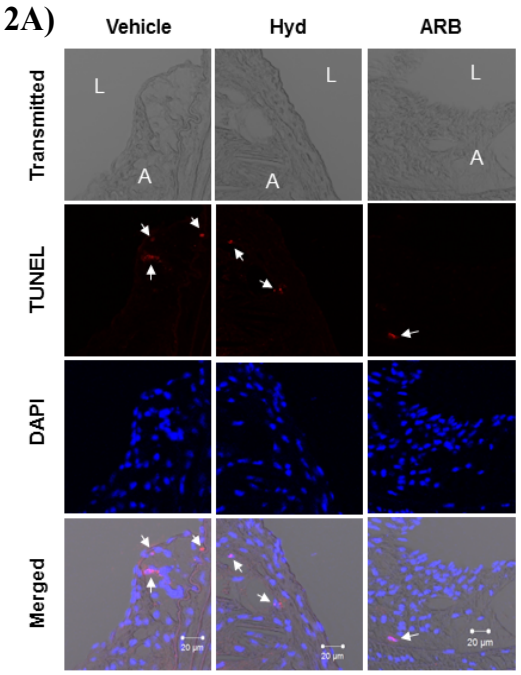


**Figure 2A: Percentage of TUNEL-positive cells is reduced in ARB treated 17-week-old ApoE$^{-/-}$ mice.**
Immunohistochemical staining of TUNEL-positive cells. Arrow indicates TUNEL-positive cells. The scale bar shows 20-μm intervals. L: lumen, A: atheroma. ARB: angiotensin receptor blocker. TUNEL: TdT-mediated dUTP nick end labeling. DAPI: 4',6-diamidino-2-phenylindole.

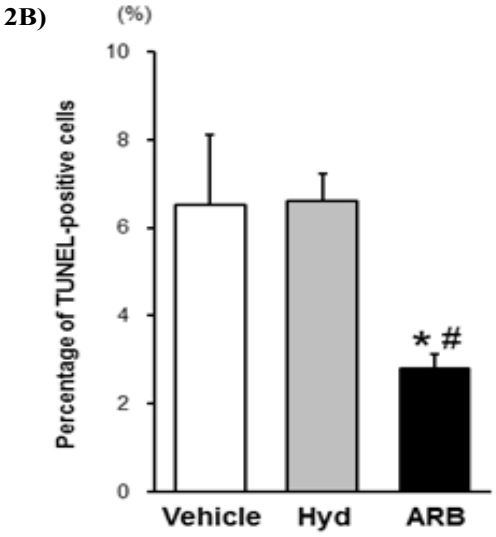


**Figure 2B:** Quantitative analysis of the percentage of TUNEL-positive cells. Values are the mean ± SE for 4 in each group. *P < 0.01 vs. vehicle-treated mice. #P < 0.01 vs. hydralazine-treated mice. Hyd: hydralazine. ARB: angiotensin receptor blocker.

inhibition by ARB could modulate CHOP mRNA expression and subsequent apoptosis. First, we isolated thioglycollate-induced peritoneal macrophages (TGPM) from wild-type mice and examined CHOP mRNA expression levels after free cholesterol (FC) loading. As shown in Figure 4A, CHOP mRNA expression showed a time-dependent increase in FC-loaded TGPMs, peaking at 8h. We therefore examined the effect of AT1R on CHOP mRNA expression at 8h after FC loading. While FC loading markedly increased CHOP mRNA expression, cotreatment with Ang II did not affect CHOP mRNA expression (Figure 4B). To exclude the possibility that AT1R counteracts with Ang II type 2 receptor (AT2R), the effects of cotreatment with Ang II plus ARB and PD123319 (a selective AT2R inhibitor) were examined. CHOP mRNA expression levels after FC loading was found to be comparable between the groups (Figure 4B). Similarly, the percentage of annexin V- or PI-positive cells after FC loading was unchanged (Figure 4C), suggesting that neither CHOP mRNA expression nor CHOP activity is autonomously regulated by AT1R or AT2R.

### AT1R-mediated oxidative stress amplifies FC-induced CHOP mRNA expression

Next, we examined the possibility that AT1R could amplify FC-

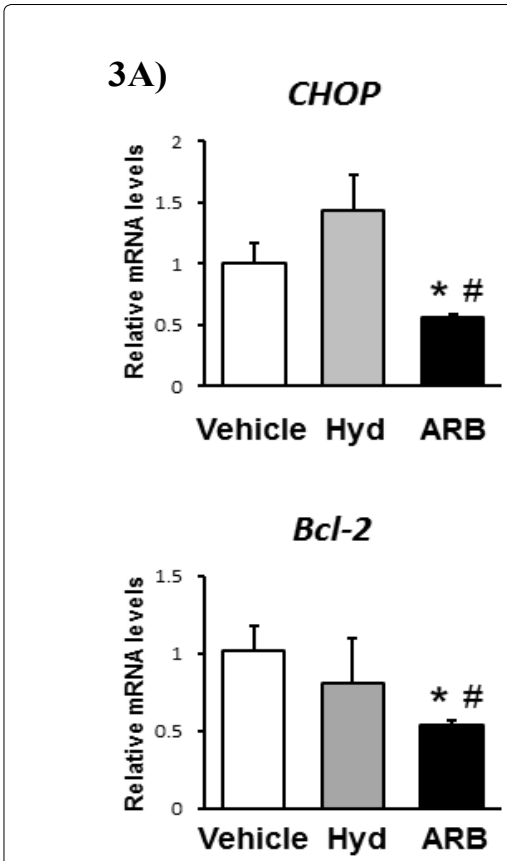


**Figure 3A: CHOP mRNA expression level is markedly attenuated in ARB-treated 17-week-old ApoE$^{-/-}$ mice**
**(A)** Quantitative PCR analysis of CHOP and Bcl-2 mRNA expression levels in brachiocephalic arteries of 17-week-old-ApoE$^{-/-}$ mice. Values are the mean ± SE relative to those in control mice. Each group consisted of 6 (vehicle), 4 (hydralazine), and 6 (ARB) mice. *P < 0.05 vs. vehicle-treated mice. #P<0.05 vs. hydralazine-treated mice. CHOP: C/EBP homologous protein. Bcl-2: B-cell lymphoma 2.

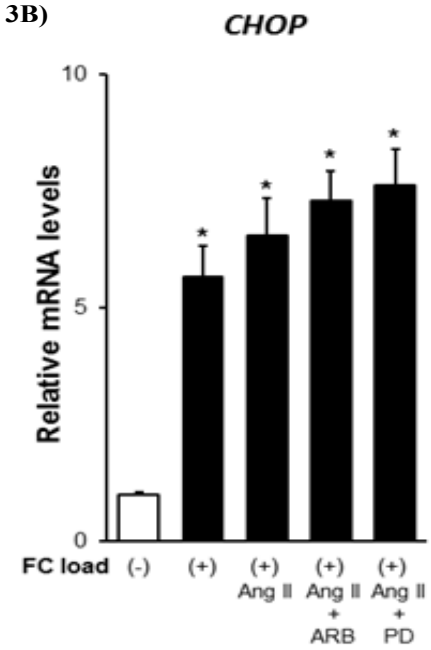


**Figure 3B:** Quantitative PCR analysis of the mRNA expression levels of Nox2 and Nox4 in the brachiocephalic artery of 17-week-old ApoE$^{-/-}$ mice. Values are the mean ± SE relative to those in vehicle-treated mice. Each group consisted of 6 (vehicle), 3 (hydralazine), and 5 (ARB) mice. *P < 0.05 vs. vehicle-treated mice. #P<0.05 vs. hydralazine-treated mice.

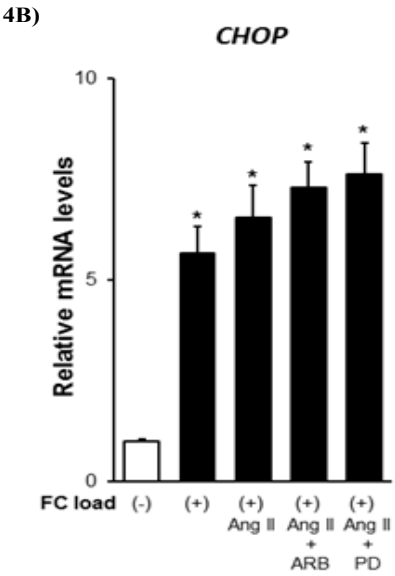


**Figure 4B:** Quantitative PCR analysis of the mRNA expression levels of CHOP in TGPMs at 8h after FC loading. Values are the mean ± SE relative to those in non-FC loaded macrophages at 8h. Each group consisted of 4 samples. Each sample was combined from 3 mice. *P<0.05 vs. TGPMs without FC loading. TGPM: thioglycollate-induced peritoneal macrophages. CHOP: C/EBP homologous protein. FC: free cholesterol. Ang II: angiotensin II. ARB: angiotensin receptor blocker. PD: PD123319, angiotensin II type 2 receptor inhibitor.

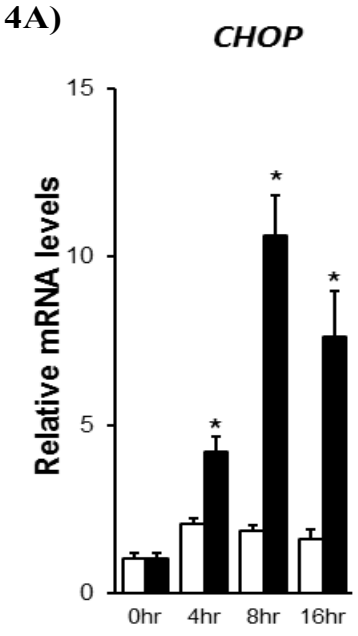


**Figure 4A: Ang II treatment does not affect the mRNA expression levels of CHOP and apoptosis in peritoneal macrophages.**
**(A)** Quantitative PCR analysis of the time-dependent mRNA expression levels of CHOP in TGPMs from wild-type mice. White bar shows TGPMs without FC loading. Black bar shows FC loaded-TGPMs. Values are the mean ± SE relative to those in TGPMs at 0h. Each group consisted of 4 samples. Each sample was combined from 3 mice. *P<0.05 vs. TGPMs at 0h. TGPM: thioglycollate-induced peritoneal macrophages. CHOP: C/EBP homologous protein. FC: free cholesterol.

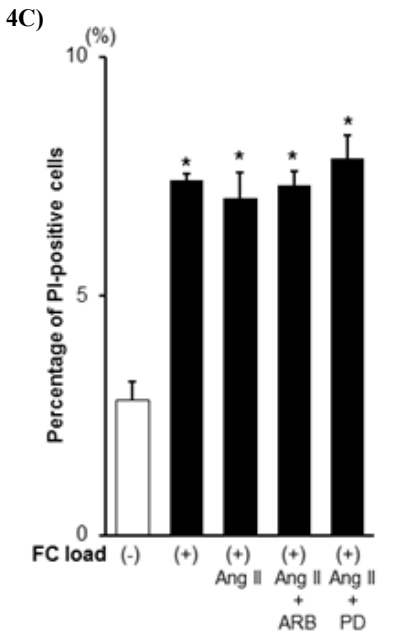


**Figure 4C:** Quantitative analysis of the percentage of annexin V or PI-positive cells in TGPMs at 16h after FC loading. Values are the mean ± SE relative to those in TGPMs without FC loading. Each group consisted of 3 samples. Each sample was combined from 3 mice. *P<0.05 vs. TGPMs without FC loading. TGPM: thioglycollate-induced peritoneal macrophages. CHOP: C/EBP homologous protein. FC: free cholesterol. Ang II: angiotensin II. ARB: angiotensin receptor blocker. PD: PD123319, angiotensin II type 2 receptor inhibitor.

induced CHOP mRNA expression by augmenting oxidative stress. We isolated TGPM from wild-type mice treated with Ang II before harvesting. Nox2 mRNA expression before FC loading was markedly increased compared with that of TGPMs from vehicle-treated mice (Figure 5A). Although Nox4 mRNA expression could not be detected in either TGPM group, mRNA expression levels of $p22^{phox}$, but not $p47^{phox}$, were significantly increased in TGPMs from Ang II-treated mice, suggesting that TGPMs from Ang II-treated mice produced more ROS than the control TGPMs. The fold increase in CHOP mRNA expression after FC loading was extensively augmented in TGPMs from Ang II-treated mice compared with that in control TGPMs (4.1-fold vs 2.0-fold, P<0.01) (Figure 5B), suggesting that AT1R amplifies CHOP mRNA expression in FC-loaded macrophages by augmenting oxidative stress.

## Discussion

In this study, we demonstrated for the first time that short-term treatment of advanced atherosclerosis lesions with ARB markedly inhibits the large necrotic core formation characteristic of rupture-prone vulnerable plaque [15,16]. We observed a significant reduction in the percentage of TUNEL-positive cells, accompanied by decreased expression of CHOP, which plays a crucial role in ER stress-induced macrophage apoptosis [23-25]. These findings suggest that AT1R profoundly contributes to necrotic core formation by promoting ER stress-induced macrophage apoptosis. Furthermore, results from *in vitro* experiments using TGPM indicated that cotreatment with Ang II does not affect FC-induced CHOP mRNA expression and subsequent apoptosis; however, the TGPM from Ang II-treated mice, with significantly increased Nox2 mRNA expression, showed exacerbated CHOP expression after FC loading. Our findings demonstrate that short-term treatment with ARB exerts an inhibitory effect on necrotic core formation in advanced plaques, which is likely to be due to the anti-oxidative effects.

Ang II has been reported to promote plaque vulnerability via AT1R activation, which is profoundly inhibited by ARB treatment in animal experiments [6-9]. Aono et al. demonstrated that AT1R deficiency or ARB treatment significantly reduced the incidence of plaque rupture in $ApoE^{-/-}$ mice [9]. They employed the murine plaque rupture model reported by Sasaki et al., in which common carotid artery was ligated followed by polyethylene cuff placement to induce neointimal cracks indicative of plaque rupture [37]. However, necrotic core and torn cap, which are key features of ruptured plaque, could not be detected in this murine model. This discrepancy between the murine model of plaque rupture and human rupture-prone plaque remains controversial [38]. We also employed the murine plaque rupture model reported by Johnson et al, in which a short period of fat feeding induced large necrotic core formation, an essential feature of rupture prone vulnerable plaque in human [38]. As the murine model of plaque rupture is poorly representative of plaque rupture in humans, especially in terms of plaque disruption and acute lumenal thrombosis, we have primarily focused on the large necrotic core formation associated with CHOP expression, which is induced by prolonged ER stress and has been reported to be closely associated with apoptosis in the human coronary artery [22]. Our findings, which demonstrate that necrotic core formation is markedly reduced by short-term treatment with ARB may provide a new insight into the regulation of rupture-prone vulnerable plaque in humans.

Ang II is known to exacerbate ER stress. The protective effect of ARB on ER stress-induced apoptosis has been reported [26-28]. Lakshmanan et al. also demonstrated that AT1R inhibition by olmesartan significantly blunted the ER stress-induced renal apoptosis in diabetic animal models [27]. Further, Wu et al. showed that CHOP expression in the myocardium of diabetic rat was inhibited by valsartan in a dose-dependent manner [28]. These experiments suggest the involvement of AT1R-mediated oxidative stress in ER stress-induced apoptosis. However, the mechanism by which AT1R exerts a direct effect on ER stress has not been addressed. Our *in vitro* experiment showing that AT1R is not autonomously implicated in CHOP gene expression and subsequent apoptosis further supports the notion that ARB treatment inhibits ER-stress induced apoptosis via the anti-oxidative effects of ARB.

Necrotic core formation is influenced by the balance between apoptosis and effective clearance of apoptotic cells by macrophages, termed efferocytosis [39-42]. Alternatively activated macrophages (M2) are the most superior efferocytic macrophage subtype [43], and the AT1R inhibitor has been reported to modulate macrophage phenotype toward M2 rather than classical activated macrophages (M1) in renal injury animal models [44,45], suggesting that the ratio of M1/M2 macrophage in ARB-treated mice is decreased, thereby contributing to the preservation of effective efferocytosis.

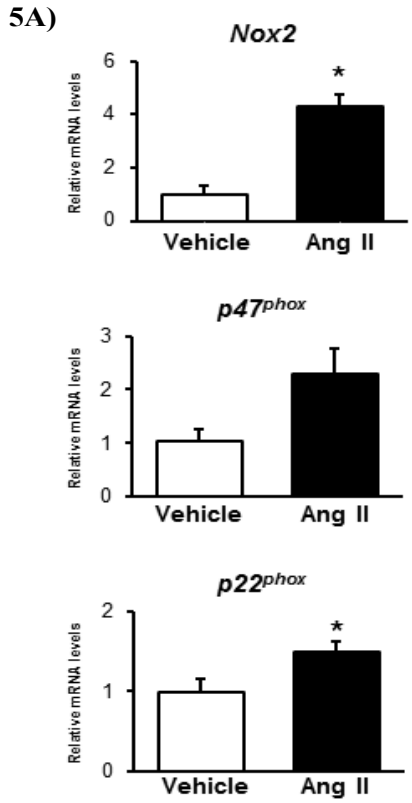


**Figure 5A: Ang II treatment does not affect the mRNA expression levels of CHOP and apoptosis in peritoneal macrophages.**
**(A)** Quantitative PCR analysis of the mRNA expression levels of Nox2, $p22^{phox}$, and $p47^{phox}$ in TGPMs from wild-type mice pretreated with Ang II or vehicle. White bar shows TGPMs from vehicle-treated mice. Black bar shows TGPMs from Ang II-treated mice. Values are the mean ± SE relative to those in TGPMs form vehicle-treated mice. Each group consisted of 3 samples. Each sample was combined from 3 mice. *P<0.05 vs. TGPMs from vehicle-treated mice. TGPM: thioglycollate-induced peritoneal macrophages.

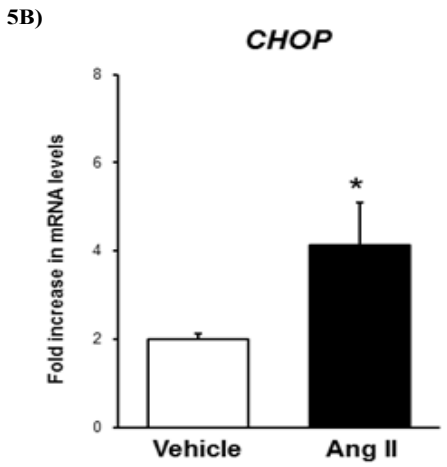


**Figure 5B:** Quantitative PCR analysis of the mRNA expression levels of CHOP in TGPMs at 8h after FC loading. White bar shows TGPMs from vehicle-treated mice. Black bar shows TGPMs from Ang II-treated mice. Values are the mean ± SE relative to those in TGPMs without FC loading in each group. Each group consisted of 3 samples. Each sample was combined from 3 mice. *P<0.05 vs. TGPMs from vehicle-treated mice. TGPM: thioglycollate-induced peritoneal macrophages. CHOP: C/EBP homologous protein. FC: free cholesterol.

Heo et al. reported that ERK5, the master regulator of molecules involved in efferocytosis, promotes efferocytosis and inhibits atherosclerosis [46]. Sharma et al. recently showed that Ang II activates ERK5 in vascular smooth muscle cells [47]. The effects of AT1R on macrophage ERK5 activation and efferocytosis need to be investigated in future studies.

The number of accumulated macrophages in the shoulder lesion has been reported to be extensively increased during the formation of vulnerable plaque [15]. Furthermore, the percentage of Mac-2-positive cells and CD68 mRNA expression levels were significantly lower in ARB-treated mice than in vehicle- and hydralazine-treated mice (Figure 1C and 1D). We previously showed that AT1R deficiency or ARB treatment attenuates differentiation/proliferation of bone marrow monocyte lineage cells and decreases the number of circulating inflammatory monocytes in ApoE$^{-/-}$ mice [48]. We therefore examined the number of circulating monocytes. Our results showed that the number of CD11b$^{+}$Ly-6C$^{high}$ circulating monocyte was significantly decreased in ARB-treated mice (Supplemental Figure 3). Further, the mRNA expression level of the MCP-1 chemokine, which is essential for the migration of circulating monocytes into plaque, was significantly reduced in ARB-treated mice (Figure 1D). On the basis of these findings, it is surmised that the decreased accumulation of inflammatory monocytes results in reduced oxidative stress in advanced plaques, thereby contributing to the attenuation of ER stress-induced apoptosis in ARB-treated mice.

In this study, we examined the Bcl-2 mRNA expression level, which has been reported to be closely involved in macrophage apoptosis in advanced atherosclerotic lesions [49]; however, recent study by Shearn et al. showed that inactivation of Bcl-x in peritoneal macrophages significantly increased the percentages of apoptotic cells after FC loading [50]. The effect of ARB on the expression levels of other apoptotic genes including proapoptotic genes like Bad and Bax should be investigated in future studies.

In conclusion, our results showed that short-term treatment with ARB in the advanced stages of atherosclerosis potentially inhibits necrotic core formation due to the anti-oxidative effects of ARB. Our findings suggest that local environmental conditions that modulate ER stress in the vessel wall are critical factors for consideration in the development of new therapeutic targets to regulate plaque vulnerability.

## Funding Sources

This work was supported by a grant from the Ministry of Education, Culture, Sports, Science and Technology of Japan.

### References

1. Yusuf S, Sleight P, Pogue J, Bosch J, Davies R, et al. (2000) Effects of an angiotensin-converting-enzyme inhibitor, ramipril, on cardiovascular events in high-risk patients. The Heart Outcomes Prevention Evaluation Study Investigators. N Engl J Med 342: 145-153.
2. Fox KM(2003) Efficacy of perindopril in reduction of cardiovascular events among patients with stable coronary artery disease: randomised, double-blind, placebo-controlled, multicentre trial (the EUROPA study). Lancet 362: 782-788.
3. Weiss D, Kools JJ, Taylor WR (2001) Angiotensin II-induced hypertension accelerates the development of atherosclerosis in apoE-deficient mice. Circulation 103: 448-454.
4. Mazzolai L, Duchosal MA, Korber M, Bouzourene K, Aubert JF, et al. (2004) Endogenous angiotensin II induces atherosclerotic plaque vulnerability and elicits a Th1 response in ApoE-/- mice. Hypertension 44: 277-282.
5. Cipollone F, Fazia M, Iezzi A, Pini B, Cuccurullo C, et al. (2004) Blockade of the angiotensin II type 1 receptor stabilizes atherosclerotic plaques in humans by inhibiting prostaglandin E2-dependent matrix metalloproteinase activity. Circulation 109: 1482-1488.
6. Suganuma E, Babaev VR, Motojima M, Zuo Y, Ayabe N, et al. (2007) Angiotensin inhibition decreases progression of advanced atherosclerosis and stabilizes established atherosclerotic plaques. J Am Soc Nephrol 18: 2311-2319.
7. Blessing E, Preusch M, Kranzhöfer R, Kinscherf R, Marx N, et al. (2008) Anti-atherosclerotic properties of telmisartan in advanced atherosclerotic lesions in apolipoprotein E deficient mice. Atherosclerosis 199: 295-303.
8. Sasaki T, Kuzuya M, Nakamura K, Cheng XW, Hayashi T, et al. (2010) AT1 blockade attenuates atherosclerotic plaque destabilization accompanied by the suppression of cathepsin S activity in apoE-deficient mice. Atherosclerosis 210: 430-437.
9. Aono J, Suzuki J, Iwai M, Horiuchi M, Nagai T, et al. (2012) Deletion of the angiotensin II type 1a receptor prevents atherosclerotic plaque rupture in apolipoprotein E-/- mice. Arterioscler Thromb Vasc Biol 32: 1453-1459.
10. Gautier EL, Huby T, Witztum JL, Ouzilleau B, Miller ER, et al. (2009) Macrophage apoptosis exerts divergent effects on atherogenesis as a function of lesion stage. Circulation 119: 1795-1804.
11. Tabas I, Seimon T, Timmins J, Li G, Lim W (2009) Macrophage apoptosis in advanced atherosclerosis. Ann N Y Acad Sci1: 40-45.
12. Seimon TA, Wang Y, Han S, Senokuchi T, Schrijvers DM, et al. (2009) Macrophage deficiency of p38alpha MAPK promotes apoptosis and plaque necrosis in advanced atherosclerotic lesions in mice. J Clin Invest 119: 886-898.
13. Tabas I (2010) Macrophage death and defective inflammation resolution in atherosclerosis. Nat Rev Immunol 10: 36-46.
14. Moore KJ, Tabas I (2011) Macrophages in the pathogenesis of atherosclerosis. Cell 145: 341-355.
15. Silvestre-Roig C, de Winther MP, Weber C, Daemen MJ, Lutgens E, et al. (2014) Atherosclerotic plaque destabilization: mechanisms, models, and therapeutic strategies. Circ Res 114: 214-226.
16. Bentzon JF, Otsuka F, Virmani R, Falk E (2014) Mechanisms of plaque formation and rupture. Circ Res 114: 1852-1866.

17. Libby P, Tabas I, Fredman G, Fisher EA (2014) Inflammation and its resolution as determinants of acute coronary syndromes. Circ Res 114: 1867-1879.

18. Lim WS, Timmins JM, Seimon TA, Sadler A, Kolodgie FD, et al. (2008) Signal transducer and activator of transcription-1 is critical for apoptosis in macrophages subjected to endoplasmic reticulum stress in vitro and in advanced atherosclerotic lesions in vivo. Circulation 117: 940-951.

19. Erbay E, Babaev VR, Mayers JR, Makowski L, Charles KN, et al. (2009) Reducing endoplasmic reticulum stress through a macrophage lipid chaperone alleviates atherosclerosis. Nat Med 15: 1383-1392.

20. Tabas I (2010) The role of endoplasmic reticulum stress in the progression of atherosclerosis. Circ Res 107: 839-850.

21. Scull CM, Tabas I (2011) Mechanisms of ER stress-induced apoptosis in atherosclerosis. Arterioscler Thromb Vasc Biol 31: 2792-2797.

22. Myoishi M, Hao H, Minamino T, Watanabe K, Nishihira K, et al. (2007) Increased endoplasmic reticulum stress in atherosclerotic plaques associated with acute coronary syndrome. Circulation 116: 1226-1233.

23. Thorp E, Li G, Seimon TA, Kuriakose G, Ron D, et al. (2009) Reduced apoptosis and plaque necrosis in advanced atherosclerotic lesions of Apoe-/- and Ldlr-/- mice lacking CHOP. Cell Metab 9: 474-481.

24. Tsukano H, Gotoh T, Endo M, Miyata K, Tazume H, et al. (2010) The endoplasmic reticulum stress-C/EBP homologous protein pathway-mediated apoptosis in macrophages contributes to the instability of atherosclerotic plaques. Arterioscler Thromb Vasc Biol 30: 1925-1932.

25. Gao J, Ishigaki Y, Yamada T, Kondo K, Yamaguchi S, et al. (2011) Involvement of endoplasmic stress protein C/EBP homologous protein in arteriosclerosis acceleration with augmented biological stress responses. Circulation 124: 830-839.

26. Xu J, Wang G, Wang Y, Liu Q, Xu W, et al. (2009) Diabetes- and angiotensin II-induced cardiac endoplasmic reticulum stress and cell death: metallothionein protection. J Cell Mol Med 13: 1499-1512.

27. Lakshmanan AP, Thandavarayan RA, Palaniyandi SS, Sari FR, Meilei H, et al. (2011) Modulation of AT-1R/CHOP-JNK-Caspase12 pathway by olmesartan treatment attenuates ER stress-induced renal apoptosis in streptozotocin-induced diabetic mice. Eur J Pharm Sci 44: 627-634.

28. Wu T, Dong Z, Geng J, Sun Y, Liu G, et al. (2011) Valsartan protects against ER stress-induced myocardial apoptosis via CHOP/Puma signaling pathway in streptozotocin-induced diabetic rats. Eur J Pharm Sci 42: 496-502.

29. Keidar S, Kaplan M, Hoffman A, Aviram M (1995) Angiotensin II stimulates macrophage-mediated oxidation of low density lipoproteins. Atherosclerosis 115: 201-215.

30. Johnson J, Carson K, Williams H, Karanam S, Newby A, et al. (2005) Plaque rupture after short periods of fat feeding in the apolipoprotein E-knockout mouse: model characterization and effects of pravastatin treatment. Circulation 111: 1422-1430.

31. Harrison DG, Cai H, Landmesser U, Griendling KK (2003) Interactions of angiotensin II with NAD(P)H oxidase, oxidant stress and cardiovascular disease. J Renin Angiotensin Aldosterone Syst 4: 51-61.

32. Cathcart MK (2004) Regulation of superoxide anion production by NADPH oxidase in monocytes/macrophages: contributions to atherosclerosis. Arterioscler Thromb Vasc Biol 24: 23-28.

33. Lassègue B, San Martín A, Griendling KK (2012) Biochemistry, physiology, and pathophysiology of NADPH oxidases in the cardiovascular system. Circ Res 110: 1364-1390.

34. Li G, Scull C, Ozcan L, Tabas I (2010) NADPH oxidase links endoplasmic reticulum stress, oxidative stress, and PKR activation to induce apoptosis. J Cell Biol 191: 1113-1125.

35. Lee CF, Qiao M, Schröder K, Zhao Q, Asmis R (2010) Nox4 is a novel inducible source of reactive oxygen species in monocytes and macrophages and mediates oxidized low density lipoprotein-induced macrophage death. Circ Res 106: 1489-1497.

36. Li B, Tian J, Sun Y, Xu TR, Chi RF, et al. (2015) Activation of NADPH oxidase mediates increased endoplasmic reticulum stress and left ventricular remodeling after myocardial infarction in rabbits. Biochim Biophys Acta 1852: 805-815.

37. Sasaki T, Kuzuya M, Nakamura K, Cheng XW, Shibata T, et al. (2006) A simple method of plaque rupture induction in apolipoprotein E-deficient mice. Arterioscler Thromb Vasc Biol 26: 1304-1309.

38. Cullen P, Baetta R, Bellosta S, Bernini F, Chinetti G, et al. (2003) Rupture of the atherosclerotic plaque: does a good animal model exist? Arterioscler Thromb Vasc Biol 23: 535-542.

39. Thorp E, Tabas I (2009) Mechanisms and consequences of efferocytosis in advanced atherosclerosis. J Leukoc Biol 86: 1089-1095.

40. Li S, Sun Y, Liang CP, Thorp EB, Han S, et al. (2009) Defective phagocytosis of apoptotic cells by macrophages in atherosclerotic lesions of ob/ob mice and reversal by a fish oil diet. Circ Res 105: 1072-1082.

41. Tabas I (2010) Macrophage death and defective inflammation resolution in atherosclerosis. Nat Rev Immunol 10: 36-46.

42. Schrijvers DM, De Meyer GR, Kockx MM, Herman AG, Martinet W (2005) Phagocytosis of apoptotic cells by macrophages is impaired in atherosclerosis. Arterioscler Thromb Vasc Biol 25: 1256-1261.

43. Zizzo G, Hilliard BA, Monestier M, Cohen PL (2012) Efficient clearance of early apoptotic cells by human macrophages requires M2c polarization and MerTK induction. J Immunol 189: 3508-3520.

44. Yamamoto S, Yancey PG, Zuo Y, Ma LJ, Kaseda R, et al. (2011) Macrophage polarization by angiotensin II-type 1 receptor aggravates renal injury-acceleration of atherosclerosis. Arterioscler Thromb Vasc Biol 31: 2856-2864.

45. Ma LJ, Corsa BA, Zhou J, Yang H, Li H, et al. (2011) Angiotensin type 1 receptor modulates macrophage polarization and renal injury in obesity. Am J Physiol Renal Physiol 300: 1203-1213.

46. Heo KS, Cushman HJ, Akaike M, Woo CH, Wang X, et al. (2014) ERK5 activation in macrophages promotes efferocytosis and inhibits atherosclerosis. Circulation 130: 180-191.

47. Sharma G, Goalstone ML (2007) Regulation of ERK5 by insulin and angiotensin-II in vascular smooth muscle cells. Biochem Biophys Res Commun 354: 1078-1083.

48. Tsubakimoto Y, Yamada H, Yokoi H, Kishida S, Takata H, et al. (2009) Bone marrow angiotensin AT1 receptor regulates differentiation of monocyte lineage progenitors from hematopoietic stem cells. Arterioscler Thromb Vasc Biol 29: 1529-1536.

49. Thorp E, Li Y, Bao L, Yao PM, Kuriakose G, et al. (2009) Brief report: increased apoptosis in advanced atherosclerotic lesions of Apoe-/- mice lacking macrophage Bcl-2. Arterioscler Thromb Vasc Biol 29: 169-172.

50. Shearn AI, Deswaerte V, Gautier EL, Saint-Charles F, Pirault J, et al. (2012) Bcl-x inactivation in macrophages accelerates progression of advanced atherosclerotic lesions in Apoe(-/-) mice. Arterioscler Thromb Vasc Biol 32: 1142-1149.

## Author Affiliations

Top

*Department of Cardiovascular Medicine, Graduate School of Medical Science, Kyoto Prefectural University of Medicine, Kyoto, Japan*